Grand canonical simulations of the interacting self-avoiding walk model

1996 J. Phys. A: Math. Gen. 29 7929

(http://iopscience.iop.org/0305-4470/29/24/017)

J. Phys. A: Math. Gen. **29** (1996) 7929–7942. Printed in the UK

Grand canonical simulations of the interacting self-avoiding walk model

Polidoros Paul Nidras†

Department of Mathematics, The University of Melbourne, Parkville, Victoria 3052, Australia

Received 5 August 1996

Abstract. We report the results obtained from simulations of the interacting self-avoiding walk (ISAW) model on the square and simple cubic lattices. In particular we verify a new scaling form for the canonical partition function in the low temperature phase as proposed by Owczarek *et al*. We also obtain estimates of the critical exponent γ_{-} in two dimensions. Finally, we obtain good agreement with previous studies on the value of a correction to scaling amplitude at the θ point on the simple cubic lattice which is in disagreement with a field theoretic prediction.

1. Introduction

The interacting self-avoiding walk (ISAW) model is a model for the collapse transition that polymers undergo in a dilute solution. In particular it is believed to possess a tricritical point which has been identified with the θ point in the corresponding polymer problem. This enables us to estimate universal quantities such as critical exponents for polymers directly from estimates of those same quantities for the model. The connection between these walk models and certain quantum field theories is another reason for studying the ISAW model.

The are three types of behaviour exhibited by polymers that are also present in the model. The self avoidance constraint causes effective excluded volume interactions between monomers. These compete with the attractive, temperature-dependent interactions that also exist between monomers. The behaviour of the model is therefore governed by the relative strengths of these two opposing forces, which are related to the entropy and to the internal energy respectively. At high temperatures the excluded volume effect dominates and the walks appear in extended configurations. At lower temperatures the attraction between monomers dominates and the walks 'collapse' into compact globule-like configurations. There is a critical point separating these two phases where the above opposing forces 'balance'. This corresponds to the θ point of real polymer systems. The fractal dimension of walks at this temperature is strictly bounded above and below by the fractal dimensions of walks in the low and high temperature phases respectively.

Of particular importance are the values of various critical exponents and other universal quantities which describe the thermal and entropic behaviour of the model both at the critical point and away from it. Using the enhanced Berretti–Sokal–Metropolis (B–S–M) algorithm [1], we are able to confirm a new scaling form for the canonical partition function in the collapsed phase of the model proposed in [2]. We also provide a plot of the free energy of the model as a function of temperature for the square and simple cubic lattices, as well as estimates for the critical exponents ν and γ.

† E-mail address: ppn@mundoe.maths.mu.oz.au

0305-4470/96/247929+14$19.50

2. The ISAW model

In this section we review some properties of SAWs and ISAWs; we also establish our notation. Let $\mathcal{L}$ be some regular d-dimensional lattice, then an n-step SAW, ψ, on $\mathcal{L}$ is a sequence of $n+1$ *distinct* points $(\psi(0), \psi(1), \ldots, \psi(n))$ such that $|\psi(i) - \psi(i+1)| = 1$. We will assume that all walks begin at the origin, i.e. $\psi(0) = \mathbf{0}$. The vertices of the lattice are commonly referred to as *sites*. A unit line segment connecting two consecutive points of the walk, $\psi(i)$ and $\psi(i+1)$, is called a *bond*. A pair of non-consecutive points on the walk that are nearest neighbours (i.e. $|\psi(i) - \psi(j)| = 1$, $j \neq i \pm 1$) is called a *nearest neighbour contact*. We can now define an ISAW by associating an energy, ϵ, with each nearest neighbour contact. It is convenient to introduce ω to be the temperature parameter†:

$$\omega = \mathrm{e}^{\epsilon/kT} \tag{1}$$

where T is the temperature and k is Boltzmann's constant. We will always choose units so that $\epsilon/k = 1$. Now we let c_n^m be the number of n-step ISAWs with m contacts starting at the origin and ending anywhere. When simulating in the grand canonical ensemble, the distribution of the walk lengths observed is governed by the canonical partition function, $Z_n(\omega)$. This function is a weighted sum over the set of all configurations ψ of fixed length n as follows:

$$Z_n(\omega) = \sum_{m \geqslant 0} c_n^m \omega^m. \tag{2}$$

The partition function is believed to exhibit two distinct types of asymptotic behaviour for large n. The first type of behaviour is well known—it is the behaviour of the partition functions for ordinary SAWs. This asymptotic form of the partition function is believed to be valid for all temperatures in the high temperature regime of the model and also at the critical point. The second behaviour has been predicted to occur in the collapsed (or low temperature) phase of the model [2] where a surface tension term also contributes to the partition function. Owczarek [3] observed this behaviour in the collapsed phase of the semi-continuous interacting partially directed self-avoiding walk model. In [2] it was conjectured that this form of the partition function for low temperatures should also be valid for the ISAW model and for real polymer systems.

The asymptotic forms for the canonical partition function are as follows:

$$Z_n^{\mathrm{high}}(\omega) \sim (\mu(\omega))^n n^{\gamma_+ - 1} \qquad n \to \infty \tag{3}$$

$$Z_n^{\mathrm{crit}}(\omega) \sim (\mu(\omega))^n n^{\gamma_t - 1} \qquad n \to \infty \tag{4}$$

$$Z_n^{\mathrm{low}}(\omega) \sim (\mu(\omega))^n \mu_s^{n^\sigma} n^{\gamma_- - 1} \qquad n \to \infty \tag{5}$$

where the subscripts used for γ indicate the temperature regime. γ_+ denotes γ in the high temperature phase of the model. It is believed to be $\frac{43}{32}$ in two dimensions [4, 5] and approximately 1.16 in three dimensions. γ_t denotes γ at the critical point and is believed to be $\frac{8}{7}$ in two dimensions [6]. It takes on its mean field value of 1 in three dimensions. Finally, γ_- is the value of γ in the collapsed phase and as far as we know, has never been estimated. It is not clear whether γ_- should be universal, or even if it is independent of temperature.

The quantity μ is called the connective constant (or effective coordination number) of the lattice $\mathcal{L}$ for SAWs ($\omega = 1$)—it is lattice dependent. For the ISAW model, μ is related to the free energy and is temperature dependent as well as lattice dependent. It can also be thought of as the *effective* connective constant of the lattice $\mathcal{L}$ at a given temperature. μ_s is

† For the sake of brevity, we will often refer to ω as the temperature even though it is a dimensionless quantity.

a quantity less than 1 and is related to the surface free energy term in the partition function that is present at low temperatures. Thus the exponent n^{σ} should have the dimension of a surface. This suggests that $\sigma = (d-1)/d$ since n is analogous to a volume. However, it is not clear whether the self avoidance constraint would lead to a reduction in σ.

We are also interested in studying the asymptotic behaviour of the 'size' of walks. This is governed by another critical exponent, ν. There are several quantities that can be used to estimate ν, but we will only use the mean-squared end-to-end distance:

$$\langle R_e^2(n)\rangle = \langle(\psi(0) - \psi(n))^2\rangle. \tag{6}$$

This quantity has the following asymptotic behaviour:

$$\langle R_e^2(n)\rangle \sim n^{2\nu} \qquad \text{as } n \to \infty \tag{7}$$

where ν takes on three different values (ν_+, ν_t and ν_-) depending on the temperature. In two dimensions ν_+ is believed [4, 5] to be $\frac{3}{4}$ and ν_t has been predicted [6] to be $\frac{4}{7}$.

It is expected that $d = 3$ is the upper critical dimension for tricritical ISAWs. This implies that the critical exponents of the model should take on their mean field values and the leading correction terms should be logarithmic. There have been several field theoretic predictions [7, 8] made about the form of these logarithmic corrections at the critical point. We check two of these predictions in this paper. The first prediction is for the canonical partition function at the critical point:

$$Z_n(\omega_t) \sim \mu_t^n \left(1 - \frac{49}{484 \ln n}\right). \tag{8}$$

The other prediction is for the mean-squared end-to-end distance:

$$R_e^2(\omega_t) \sim n \left(1 - \frac{37}{363 \ln n}\right). \tag{9}$$

There are many other quantities that can also be examined for the ISAW model (such as the specific heat), however most of these are best simulated at fixed n, i.e. in the canonical ensemble.

3. The algorithm

The B–S algorithm [9] simulates SAWs in a grand canonical ensemble at fixed monomer fugacity, z, with one endpoint fixed at the origin and the other endpoint free. Each n-step walk has a probability of $z^n/G(z)$ of appearing in the ensemble, where

$$G(z) = \sum_{n=0}^{\infty} c_n z^n \tag{10}$$

is the grand partition function and c_n is the number of n-step SAWs. The B–S algorithm is similar to the Redner–Reynolds algorithm [10] and also Grassberger's algorithm [11, 12] which are both incomplete enumeration algorithms. Its main advantage over these two algorithms is that it is a well-defined, dynamic, Markov process, rather than a stochastic enumeration procedure. This means that the large amount of effort put into understanding the correlations in the data of other dynamic Monte Carlo algorithms can also be applied to this algorithm. The situation for the quasi-static algorithms mentioned above is quite different since the correlations in the data generated by these algorithms are not well understood. This can result in the underestimation of statistical errors in the data, possibly leading to erroneous estimates of confidence intervals.

The simulation of ISAWs with the B–S algorithm is easily achieved by including a standard Metropolis accept/reject step. This introduces the parameter ω defined in section 2 which allows the temperature to be controlled. Thus the grand partition function for the simulation of ISAWs is

$$G(z,\omega)=\sum_{n=0}^{\infty} z^n Z_n(\omega). \tag{11}$$

When we first implemented the algorithm, we found that it became increasingly inefficient as ω was increased. For values of ω corresponding to the collapsed phase of the model, the autocorrelation times of our observables were very large. This led us to modify the basic move of the algorithm in an attempt to lower these autocorrelation times—we achieved a reasonable reduction for low temperatures (about a factor of 2). Below we briefly present the details of the B–S–M algorithm along with this new local move; for more specific details, see [1].

The B–S algorithm consists of two basic moves: appending a bond onto the end of the walk, or deleting a bond from the end of the walk. These moves have to be chosen with the correct relative probabilities in order to satisfy detailed balance. To simulate ISAWs, we add in the standard Metropolis move; we call this the B–S–M algorithm. In [1] it was shown that adding/deleting a *walk* of length Δn rather than a single bond can improve the efficiency of the algorithm. Unfortunately the gain in efficiency deteriorates as the temperature is lowered, especially in two dimensions. We attempted to improve the efficiency of the algorithm near the critical point by introducing a scheme which varied the length of the walks to be added/deleted. This scheme was partly successful and we used it for several temperatures in the two-dimensional simulations.

In order to carry out the simulations, we needed to decide on the average length of walks that would be simulated and also the temperature values to be simulated. These two considerations are not independent of each other, so a large number of test runs were performed at various ω values to tune the fugacity z which controls the lengths of the walks being simulated. The other quantity which came into consideration when choosing $\langle n\rangle$ was the autocorrelation time of the observables.

Some additional caution was required when choosing the parameter values for the low temperature grand canonical simulations. This is due to the singularity structure of the generating function, $G(z,\omega)$ [13]. The radius of convergence of the generating function consists of a line of simple singularities at high temperatures which are dominated by an algebraic singularity. At low temperatures, there is an infinite accumulation of poles at the radius of convergence which results in a line of essential singularities. Moreover, the generating function (and hence $\langle n\rangle$) is finite on the radius of convergence. The line of algebraic singularities and the line of essential singularities meet at the tricritical point, ω_c (see figure 3 of [13]).

The line of essential singularities in the low temperature phase produced instability in the simulations. The instability made it difficult to know whether or not we were simulating in the unphysical regime $z > z_c$. This problem was overcome by performing the simulations for some value of z and subsequently estimating z_c from the data. The simulation was taken to be valid if it was self-consistent, i.e. if z was found to be less than the estimate of z_c. This method worked well in two dimensions but the simulations in the low temperature regime on the simple cubic lattice proved to be rather difficult; this is reflected in the results we obtained for that lattice.

An additional problem that we experienced for the low temperature simulations was that only small values of $\langle n\rangle$ could be simulated. This effect was particularly severe in

three dimensions, as can be seen in section 5. One way to 'boost' the value of $\langle n \rangle$ for low temperatures is to simulate in a slightly different ensemble whose generating function is:

$$G_p(z, \omega) = \sum_{n=0}^{\infty} z^n n^p Z_n(\omega) \tag{12}$$

where the parameter p is some small integer. The simulation of this ensemble can be achieved by making the appropriate changes to the transition probabilities of the Markov chain.

Our main task of verifying the proposed new form of the partition function in the low temperature phase was achieved by recording the grand canonical n-distribution generated by the runs. Our method was to attempt to fit a curve to the observed distribution and to subsequently test the goodness of this fit by using a χ^2 test. The mean squared end-to-end distance was also collected canonically and this allowed us to estimate the exponent ν.

4. Results: two dimensions

We carried out simulations at 18 different temperatures, five of which were in the effective low temperature regime. Since our simulations were carried out for rather small values of n, we needed a criterion to determine the effective temperature regime in which we were simulating. The low temperature regime was taken to be the range of ω values where the effective exponent ν was found to be less than 0.5. All of the high temperature simulations, including those at the effective critical point, used $\langle n \rangle \approx 300$. The sample sizes ranged from 1×10^6 to 3.7×10^7 independent configurations for the simulations in the high temperature regime and at the critical point. The values for $\langle n \rangle$ used in the low temperature regime ranged from 200 at $\omega = 2.0$ to 100 at $\omega = 2.2$. The larger autocorrelation times for observables in the collapsed phase meant that our sample sizes were limited to 1×10^6 independent configurations.

Table 1. Parameters values for simulations in two dimensions.

ω	z	$\langle n \rangle$	Δn	Scheme	Sample size	$\tau_{\mathrm{int},n}$
1.0	0.3773	300	14	M	3.7×10^7	2600
1.1	0.3713	300	14	M	1×10^7	4500
1.2	0.365	300	14	M	1×10^7	4800
1.3	0.358 32	300	14	M	1×10^7	6500
1.4	0.3514	300	14	M	6×10^6	8500
1.5	0.344 28	300	10	M	5×10^6	17 000
1.6	0.336 92	300	8	M	4.1×10^6	28 000
1.7	0.329 33	300	8	Q	2×10^6	45 000
1.8	0.321 22	300	8	L	2×10^6	150 000
1.9	0.312 84	300	5	L	1×10^6	140 000
1.94	0.3094	300	5	L	1.5×10^6	140 000
1.945	0.309 02	300	5	L	3.6×10^6	220 000
1.95	0.308 55	300	6	L	1×10^6	220 000
2.0	0.3036	200	4	M	1×10^6	165 000
2.05	0.2993	200	3	M	1×10^6	340 000
2.1	0.2945	150	3	M	1×10^6	280 000
2.15	0.2895	100	3	M	8.8×10^5	240 000
2.2	0.2852	100	4	L	1.05×10^6	320 000

Table 1 shows ω for each simulation, the value of the fugacity, z, which was chosen for each temperature and the corresponding average length of walks that were simulated at each temperature. An M in the scheme column means that Δn was fixed in the simulation at the value displayed in the Δn column. An L or Q in the scheme column means that Δn was allowed to vary for each Monte Carlo step. This was achieved by choosing the maximum possible value of Δn allowed, call it k (this is the number in the Δn column). A weight was then prescribed for all walk lengths up to k and for each Monte Carlo step, a walk length was randomly chosen according to the weights. For the L scheme, the weights w_i were

$$w_i = \frac{i}{\sum_{j=1}^{k} j} \tag{13}$$

while for the Q scheme they were

$$w_i = \frac{i^2}{\sum_{j=1}^{k} j^2}. \tag{14}$$

The last column in table 1 shows an estimate of the integrated autocorrelation time, $\tau_{\mathrm{int},n}$, for the observable n. This quantity is defined as the area under the autocorrelation function, $C_{nn}(s)$. We used the procedure suggested in appendix C of [14] to obtain the estimates presented in table 1.

4.1. Estimating μ, γ and μ_s

The B–S–M algorithm generates a correlated sequence of ISAWs in the grand canonical ensemble at fixed monomer fugacity z and temperature ω. Each ISAW appears in this sequence with probability $z^n\omega^m/G(z,\omega)$ where $G(z,\omega)$ is the grand partition function given in (11).

A more practical quantity to consider is the probability of *any* walk of length n appearing in the sample (i.e. the distribution of the walk lengths generated by the algorithm in the grand canonical ensemble) which is given by $z^n Z_n(\omega)/G(z,\omega)$. This is useful because we can use (3), (4) or (5) to approximate $Z_n(\omega)$. Since z and ω are constant in our simulations, $G(z,\omega)$ will also be constant so we do not have to estimate the form of the grand partition function. The distribution of the walk lengths can be directly collected from the run by producing a histogram for n.

We can estimate μ, γ and μ_s by assuming the histograms are given exactly by either

$$H_{z,\omega}(n) = A(\mu z)^n n^{\gamma-1} \tag{15}$$

for simulations in the high temperature phase and at the critical point, or

$$H_{z,\omega}(n) = A(\mu z)^n \mu_s^{n^\sigma} n^{\gamma-1} \tag{16}$$

for simulations in the low temperature phase. Of course (15) and (16) only describe the leading asymptotic behaviour for $H_{z,\omega}(n)$. We followed the procedure described in [9] to deal with correction to scaling terms. For ISAWs at high temperatures we used the following form:

$$H_{z,\omega}(n) = A(\mu z)^n (n+k)^{\gamma-1} \tag{17}$$

where k is some small fixed number.

In order to obtain estimates for μ and γ in the high temperature phase and at the critical point, we introduce a cut-off parameter, $n_{\min}$. The curve fitting was then performed for a range of k and $n_{\min}$ values. The best estimates were considered to be those that satisfied

the *flatness criterion*, i.e. where the dependence of the estimates on $n_{\min}$ were the weakest. In general there was a range of k values that yielded reasonably flat curves for μ and γ. We will refer to the range of values for μ and γ which satisfied the flatness criterion as the systematic error. The statistical error on the other hand was provided by the fitting method that was used. We used two fitting methods—the maximum likelihood procedure that is outlined in [9] and also nonlinear regression.

The procedure we used for estimating μ, γ and μ_s in the low temperature phase was somewhat different to that used for the high temperature phase. First we assumed that σ took the value of $(d-1)/d$, where d is the lattice dimension. If we did not do this, we would have had to perform a five-parameter fit which would have led to unacceptably large error bars—especially for σ and γ. We did not estimate the systematic error in the low temperature phase because the statistical error was at least several times larger.

4.2. Verifying new scaling form

We used the χ^2 test to determine the goodness of the fit of (16) to the actual histograms produced by the simulations. We first calculated the χ^2 value of the fit:

$$\chi^2 = \sum_{n=n_{\min}}^{M} \frac{(H_{z,\omega}(n) - O_{z,\omega}(n))^2}{H_{z,\omega}(n)} \tag{18}$$

where $O_{z,\omega}(n)$ are the observed values of the histograms and M is the maximum number of data points. Since $(M - n_{\min}) \gg 30$, we can approximate the χ^2 distribution by a normal distribution with unit variance and a mean of $\sqrt{2\chi^2} - \sqrt{2p-1}$, where $p = (M - n_{\min}) - 4$ is the number of degrees of freedom. We use this distribution to determine the *significance level*, which is the probability that χ^2 would exceed the value calculated in (18). A small significance level of less than, say 5%, would indicate a problem with the fit, although it would not necessarily rule out the fitting function.

4.3. Estimating ν

We chose to estimate ν from our simulations by analysing our data canonically, i.e. we estimated $\langle R_e^2(n) \rangle$ by averaging the observable R_e^2 at fixed n. We then performed a weighted least squares fit by assuming that

$$\langle R_e^2 \rangle = A(n+k)^{2\nu} \tag{19}$$

was exact for all $n > n_{\min}$, where k is some small fixed number. Another assumption in using (19) is that the exponent of the leading correction term is at most -1 (this is not believed to be true for three dimensional SAWs). We used the flatness criterion mentioned previously to determine our best estimate of ν. The range of values of ν for those curves that satisfied the flatness criterion was taken as an estimate of the systematic error.

4.4. Numerical results

In all of the estimates stated in this paper, we will adopt the following convention.

- All of the statistical errors stated will be 95% confidence intervals, i.e. 2 standard deviations.
- If two error bars are given for an estimate, then the format is: central estimate $\pm$ statistical error $\pm$ systematic error.
- If one error bar is given, then the format is: central estimate $\pm$ statistical error.

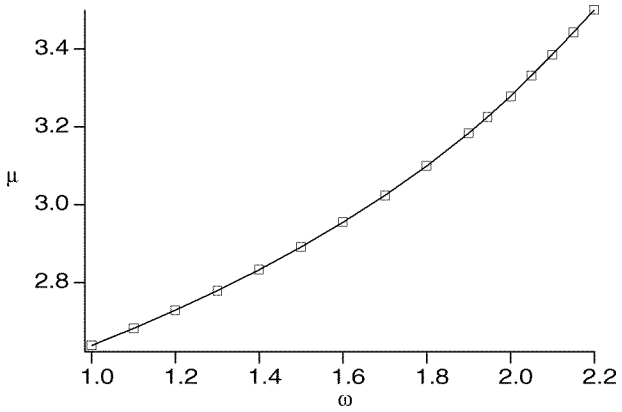

Figure 1. μ against ω for the square lattice.

Figure 1 shows the plot of $\mu(\omega)$ for the square lattice. The error bars for the estimates of μ are smaller than the symbols used on the graph. We performed two estimates for μ at $\omega = 1$ (i.e. for SAWs)—assuming that $\gamma = \frac{43}{32}$ gives:

$$\mu_{\mathrm{SAW}} = 2.638\,154 \pm 0.000\,010 \pm 0.000\,007 \tag{20}$$

whilst with γ as a free parameter we find that:

$$\mu_{\mathrm{SAW}} = 2.638\,164 \pm 0.000\,004 \pm 0.000\,010. \tag{21}$$

Both of these results are consistent with recent enumeration data [15], however the central estimate of the fit that assumed $\gamma = \frac{43}{32}$ was closer to the estimate for μ obtained via enumeration.

Tables 2 and 3 show our estimates for γ and ν. The case $\omega = 1$ corresponds to the SAW model and we obtain excellent agreement with the conjectured values of both γ_+ and ν_+. Note that the systematic error in the estimate of γ_+ is actually larger than the corresponding statistical error.

We indirectly estimated the critical point, ω_t, in two ways. We assumed that ω_t occurs when γ and ν take on their predicted values of $\frac{8}{7}$ and $\frac{4}{7}$ respectively. A simple linear interpolation of the data from table 2 yields a central value of 1.943 for ω_t. A similar fit to the data in table 3 yields $\omega_t = 1.946$. Both of these results are in excellent agreement

Table 2. γ in two dimensions for all three temperature regimes.

ω	Regime	γ
1.0	γ_+	$1.3414 \pm 0.0011 \pm 0.0015$
1.94		$1.157 \pm 0.010 \pm 0.007$
1.945	γ_t	$1.132 \pm 0.005 \pm 0.004$
1.95		$1.106 \pm 0.009 \pm 0.005$
2.0		1.06 ± 0.03
2.05		1.11 ± 0.03
2.10	γ_-	1.07 ± 0.04
2.15		1.09 ± 0.08
2.20		1.11 ± 0.06

Table 3. ν in two dimensions for SAWs and at the critical point.

ω	Regime	ν
1.0	ν_+	$0.7499 \pm 0.0003 \pm 0.0002$
1.94		$0.5797 \pm 0.0028 \pm 0.0017$
1.945	ν_t	$0.5727 \pm 0.0011 \pm 0.0007$
1.95		$0.5667 \pm 0.0026 \pm 0.0019$

with the results of [11] (they get $\omega_t = 1.944 \pm 0.004$) and are consistent with each other. We use these estimates of ω_t to estimate μ_t:

$$\mu_t = 3.224 \pm 0.004. \tag{22}$$

The relatively large error in this estimate is mainly due to the uncertainty of the critical point.

The lower half of table 2 contains estimates of γ in the collapsed phase of the model with 95% confidence intervals. Despite the large error bars, the fluctuations of the estimates for γ as a function of $n_{\min}$ were surprisingly small. We observed oscillatory behaviour for γ in the low temperature phase up to $n_{\min} \approx 35$. This suggests that using enumeration data to estimate γ_- would be very difficult to analyse as the oscillations were quite large. We suspect that the low estimate for γ at $\omega = 2.0$ may be a crossover effect so we excluded it from our final calculation of γ_-. The large error bar obtained for $\omega = 2.15$ was due to unusually large oscillations for small values of $n_{\min}$. As a result, we had to throw away more data than usual for our estimate of γ at this temperature.

From the data presented in table 2, it is not clear whether or not γ_- is dependent on temperature. We would have to perform much larger simulations at lower temperatures to confirm or refute this. However, there does not appear to be a trend in the central estimates. Thus it is possible that the variations are due to purely statistical errors in which case we can estimate γ_- by averaging these estimates. We performed a weighted average of the data points, apart from $\omega = 2.0$, and our estimate for γ_- is:

$$\gamma_- = 1.095 \pm 0.045. \tag{23}$$

The inclusion of $\omega = 2.0$ in the average, results in a slightly smaller central estimate: $\gamma_- = 1.085 \pm 0.04$.

We now check the validity of the proposed new form (5) for the canonical partition function in the low temperature phase. All of the tests that we carried out assumed $\sigma = \frac{1}{2}$ in two dimensions and $\sigma = \frac{2}{3}$ in three dimensions. Table 4 shows the results of the χ^2

Table 4. χ^2 and significance levels of the curve fitting for the partition function at low temperatures in two dimensions.

ω	$n_{\min}$	Degrees of freedom	χ^2	Level
2.0	44	509	526.0	29%
2.05	60	847	812.4	79%
2.10	66	669	688.8	28%
2.15	57	500	498.2	51%
2.20	119	828	866.2	17%

Table 5. μ_s as a function of ω in two dimensions.

ω	μ_s
2.0	0.978 ± 0.014
2.05	0.925 ± 0.007
2.10	0.893 ± 0.016
2.15	0.83 ± 0.022
2.20	0.80 ± 0.013

tests that we performed for each ω. We argue that these tests taken together demonstrate convincingly the validity of (5), at least for $d = 2$. We found that large contributions were made to χ^2 for very small and very large values of n. The large residuals observed for small n values were due to correction to scaling terms. We dealt with these by introducing a cut-off parameter, $n_{\min}$, as can be seen in (18). The large contributions to χ^2 from the tail of the distribution, where the statistics are poor, were also cut off by reducing M. We attribute the small significance level at $\omega = 2.2$ to poor statistics. Since the average length of the walks generated by the algorithm at this temperature was smaller, a greater proportion of the data was lost to reduce the effects of correction terms. We did, however, plot the residuals for $\omega = 2.2$ and could find no significant trends.

Table 5 shows the estimates of μ_s that were obtained from the curve fitting. These estimates are encouraging since, as expected, they decrease steadily with increasing ω. We also estimated μ_s at $\omega = 1.95$—just below the critical point and we found it to be 1 within error bars. The behaviour of μ_s close to the critical point has been conjectured [13] to be characterized by the critical exponent, χ (not to be confused with χ^2 of (18)):

$$|1 - \mu_s| \sim |\omega - \omega_t|^{\chi} \qquad \text{as } \omega \to \omega_t \tag{24}$$

where it is believed that $\chi = \sigma/\phi = \frac{7}{6}$ in two dimensions. Our estimates for μ_s are too crude to attempt to verify this relation—it may also be necessary to perform simulations much closer to the critical point to estimate χ.

5. Results: three dimensions

The simulations in three dimensions were performed at 12 different temperatures with four of these in the low temperature phase. All of the high temperature simulations were performed at $\langle n \rangle \approx 300$. The sample sizes ranged from 5×10^6 to 1×10^7 independent samples in the high temperature phase and at the critical point. The simulations in the low temperature phase were performed from $\langle n \rangle = 300$ at $\omega = 1.325$ to $\langle n \rangle = 80$ at $\omega = 1.375$. The sample sizes in the low temperature phase ranged from 5×10^6 to 4×10^7 independent samples. It was not possible to simulate at lower temperatures or at larger $\langle n \rangle$ due to the instability that was described in section 3. The parameter values that were chosen for the runs on the simple cubic lattice are displayed in table 6.

We used the procedure described in section 4.1 to obtain estimates for μ, γ and μ_s. However, since $d = 3$ is the upper critical dimension for tricritical ISAWs, we had to insert a logarithmic correction term for the behaviour of the histograms, i.e. we modified (17) to

$$H_{z,\omega}(n) = A(\mu z)^n n^{\gamma - 1} \left(1 + \frac{D}{\ln n}\right) \tag{25}$$

Table 6. Parameter values for simulations in three dimensions.

ω	z	$\langle n \rangle$	Δn	Scheme	Sample size	$\tau_{\mathrm{int},n}$
1.0	0.212 68	300	9	M	1×10^7	5500
1.05	0.2105	300	9	M	5×10^6	4900
1.1	0.208 25	300	9	M	1×10^7	5800
1.15	0.2059	300	9	M	5×10^6	5700
1.2	0.203 44	300	9	M	1×10^7	7600
1.25	0.2008	300	9	M	5×10^6	8000
1.3	0.197 97	300	9	M	5×10^6	16 000
1.31	0.197 37	300	9	M	5×10^6	17 000
1.325	0.196 44	300	9	M	5×10^6	26 300
1.35	0.194 53	200	8	M	5×10^6	17 800
1.365	0.193	120	8	M	1×10^7	14 000
1.375	0.1917	80	5	M	4×10^7	5300

for $\omega = \omega_t$. A similar correction term was used for the estimation of ν_t:

$$\langle R_e^2(n) \rangle = A n^{2\nu_t} \left(1 + \frac{E}{\ln n} \right). \tag{26}$$

For ordinary SAWs in three dimensions, there is evidence from simulations and from renormalization group arguments [17] that the exponent of the leading correction term is -0.5. Thus we we also modified (19) to estimate ν_+:

$$\langle R_e^2(n) \rangle = A n^{2\nu_+} \left(1 + \frac{F}{n^{0.5}} \right). \tag{27}$$

5.1. Numerical results

Figure 2 shows $\mu(\omega)$ for the simple cubic lattice. Our estimate for the connective constant for the simple cubic lattice is:

$$\mu_{\mathrm{SAW}} = 4.684\,07 \pm 0.000\,04 \pm 0.000\,02. \tag{28}$$

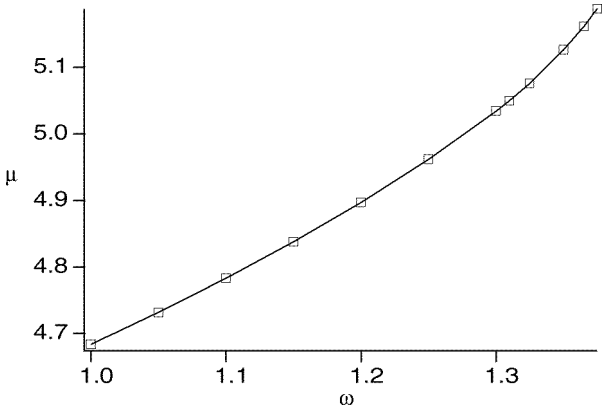

Figure 2. μ against ω for the simple cubic lattice.

Table 7. γ in three dimensions for all three temperature regimes.

ω	Regime	γ
1.0	γ_+	$1.1581 \pm 0.0025 \pm 0.0033$
1.31	γ_t	$0.9985 \pm 0.0035 \pm 0.0033$
1.325		0.997 ± 0.018
1.35		1.036 ± 0.025
1.365	γ_-	1.08 ± 0.05
1.375		1.14 ± 0.12

This estimate is larger than the value obtained in [16], although there is some overlap in the error bars. We also performed one simulation at $\omega = 1.31$ which should be close to the critical point where we find

$$\mu(\omega = 1.31) = 5.050\,02 \pm 0.000\,05 \pm 0.000\,03 \tag{29}$$

which is in good agreement with that of [12].

Table 7 contains our estimates for γ for all three temperature regimes. Our value for γ_+ is significantly smaller than the value stated in [16], although the error bars do overlap. Note that the systematic error is larger than the statistical error. The estimate for γ at $\omega = 1.31$ is essentially 1 within error bars, which is the mean field value of γ. This result supports the estimate of ω_t in [12] (i.e. $\omega_t = 1.3083 \pm 0.0006$). Note that we also obtain $\gamma = 1$ within error bars at $\omega = 1.325$; however, at this value of ω, $\mu_s < 1$ (see table 9) which suggests that this is not the critical point.

The use of (25) in determining μ and γ around the critical point also enabled us to check (8). If (8) is indeed true, then we would expect the flatness criterion to be valid for $D \approx -49/484 \approx -0.101$. The values of D in our analysis which produced curves that satisfied the flatness criterion at $\omega = 1.31$ were -0.17 ± 0.07. The field theoretic prediction lies inside our error bars, so it cannot be ruled out. Our result for D is in reasonable agreement with Grassberger and Hegger's result (here D is given by the slope of the curve corresponding to $\omega = 1.31$ in figure 21 of [12], which we estimate to be approximately -0.22).

The lower section of table 7 contains our estimates for γ in the collapsed phase of the model. The data suggests that $\gamma_- > 1$, but that is just about all that we can conclude from it. Much larger simulations at lower temperatures would be necessary to determine the true behaviour of γ_-.

We performed a weighted least squares fit of $\langle R_e^2 \rangle$ against n using (27). This resulted in

$$\nu_+ = 0.5882 \pm 0.0007 \pm 0.0010 \tag{30}$$

which is in good agreement with the result of [17]. When estimating ν_t around the critical point we used the logarithmic correction term of (26). This yielded

$$\nu_t = 0.5001 \pm 0.0012 \pm 0.0019 \tag{31}$$

which is in excellent agreement with the expected mean field value of 0.5. Fitting (26) to the squared end-to-end distance data also enabled us to check the field theoretic prediction given in (9). Grassberger and Hegger's simulations completely ruled out this prediction since the slope of the curve in figure 18 of [12] is approximately -0.73. We obtain $E = -0.66 \pm 0.06$

Table 8. χ^2 and significance levels of the curve fitting for the partition function at low temperatures in three dimensions.

ω	$n_{\min}$	Degrees of freedom	χ^2	Level
1.325	216	413	465.0	4%
1.35	126	378	409.4	13%
1.365	112	155	180.4	8%
1.375	85	174	188.0	22%

Table 9. μ_s as a function of ω in three dimensions.

ω	μ_s
1.325	0.996 ± 0.002
1.35	0.978 ± 0.003
1.365	0.962 ± 0.006
1.375	0.946 ± 0.012

from our simulations which is in reasonable agreement with Grassberger and Hegger's result and hence in complete disagreement with the field theoretic prediction.

Table 8 shows the results of the χ^2 tests we performed for the curve fits. All of the results produced small significance levels; however, we found that a lot of the contribution to χ^2 came from the tail of the distribution except for $\omega = 1.325$. We believe that the poor results that we obtain for the fit of the histograms at $\omega = 1.325$ to (16) are probably due to a logarithmic correction term since this point is close to the critical point. A plot of the residuals for $\omega = 1.325$ show no apparent trends for n up to 3000. We also performed plots of the residuals for the other temperatures and found that they were small and randomly fluctuating around zero for n up to about 1000. For $n > 1000$, the residuals became large as the statistics in that regime were poor. There was a small upward trend in the residuals for large n at $\omega = 1.365$ and $\omega = 1.375$ which indicates that the curve fit underestimated the histograms in the tail of the distribution.

Our estimates for μ_s are given in table 9. We find once more that μ_s decreases steadily for increasing ω. We also calculated μ_s closer to the critical point at $\omega = 1.31$ and as in two dimensions, we obtained a result very close to 1. The value of the exponent χ in three dimensions is expected to be $\sigma/\phi = \frac{4}{3}$, but once again our data is too noisy to attempt to verify this.

6. Conclusion

We simulated the ISAW model using the B–S–M algorithm on the square and simple cubic lattices. Our results confirm the validity of a new scaling form for the canonical partition function in the low temperature phase of the model in $d = 2$. The results for $d = 3$ were not as convincing since we could not simulate sufficiently long walks in the low temperature phase using the grand canonical ensemble. To simulate longer walks, a slightly different ensemble would have to be used, such as the one associated with (12). Our simulations also allowed us to estimate γ_- for both lattices. It is not clear from the data whether or not γ_- is dependent on temperature. However, our data suggests that $\gamma_- > 1$ for the ISAW model on

the square and simple cubic lattices. As a consistency check, we have also estimated other quantities that have been examined in previous studies and have obtained good agreement with them. In particular, we found that our estimate of the correction to scaling amplitude of the end-to-end distance at the θ point on the simple cubic lattice was in disagreement with a prediction from field theory.

Acknowledgments

I would like to thank Dr Richard Brak for many useful and illuminating discussions, without which this work would not have been possible. I would also like to thank Richard Brak and Aleks Owczarek for critically reading the manuscript. I am grateful to the School of Graduate Studies at the University of Melbourne for an Australian Postgraduate Award.

References

[1] Nidras P P and Brak R *J. Phys. A: Math. Gen.* submitted
[2] Owczarek A L, Prellberg T and Brak R 1993 *Phys. Rev. Lett.* **70** 951
[3] Owczarek A L 1993 *J. Phys. A: Math. Gen.* **26** L647
[4] Nienhuis B 1982 *Phys. Rev. Lett.* **49** 1062
[5] Nienhuis B 1987 *Phase Transitions and Critical Phenomena* vol 11, ed C Domb and J L Lebowitz (London: Academic)
[6] Duplantier B and Saleur H 1987 *Phys. Rev. Lett.* **59** 539
[7] Duplantier B 1986 *Europhys. Lett.* **1** 491
[8] Duplantier B 1987 *J. Chem. Phys.* **86** 5293
[9] Berretti A and Sokal A D 1985 *J. Stat. Phys.* **40** 485
[10] Redner S and Reynolds P J 1981 *J. Phys. A: Math. Gen.* **14** 2679
[11] Grassberger P and Hegger R 1995 *J. Physique* I **5** 597
[12] Grassberger P and Hegger R 1995 *J. Chem. Phys.* **102** 6881
[13] Brak R, Owczarek A L and Prellberg T 1993 *J. Phys. A: Math. Gen.* **26** 4565
[14] Madras N and Sokal A D 1987 *J. Stat. Phys.* **50** 109
[15] Guttmann A J Private communication
[16] Grassberger P 1993 *J. Phys. A: Math. Gen.* **26** 2769
[17] Li B, Madras N and Sokal A D 1995 *J. Stat. Phys.* **80** 661